Polymer 51 (2010) 2360–2367

Contents lists available at ScienceDirect

Polymer

journal homepage: www.elsevier.com/locate/polymer

Graphitic carbon nanofibers developed from bundles of aligned electrospun polyacrylonitrile nanofibers containing phosphoric acid

Zhengping Zhou [a], Kunming Liu [a], Chuilin Lai [b], Lifeng Zhang [b], Juanhua Li [a], Haoqing Hou [a,*], Darrell H. Reneker [c], Hao Fong [b,**]

[a] College of Chemistry and Chemical Engineering, Jiangxi Normal University, Nanchang, Jiangxi 330027, China
[b] Department of Chemistry, South Dakota School of Mines and Technology, Rapid City, SD 57701, USA
[c] Department of Polymer Science, University of Akron, Akron, OH 44325, USA

ARTICLE INFO

Article history:
Received 12 December 2009
Received in revised form
20 March 2010
Accepted 25 March 2010
Available online 31 March 2010

Keywords:
Electrospinning
Graphitic carbon nanofibers
Polyacrylonitrile

ABSTRACT

Graphitic carbon nanofibers (GCNFs) with diameters of approximately 300 nm were developed using bundles of aligned electrospun polyacrylonitrile (PAN) nanofibers containing phosphoric acid (PA) as the innovative precursors through thermal treatments of stabilization, carbonization, and graphitization. The morphological, structural, and mechanical properties of GCNFs were systematically characterized and/or evaluated. The GCNFs made from the electrospun PAN precursor nanofibers containing 1.5 wt.% of PA exhibited mechanical strength that was 62.3% higher than that of the GCNFs made from the precursor nanofibers without PA. The molecules of PA in the electrospun PAN precursor nanofibers initiated the cyclization and induced the aromatization during stabilization, as indicated by the FT-IR and TGA results. The stabilized PAN nanofibers possessed regularly oriented ladder structures, which facilitated the further formation of ordered graphitic structures in GCNFs during carbonization and graphitization, as indicated by the TEM, XRD, and Raman results.

1. Introduction

Polyacrylonitrile (PAN) based carbon fibers have been the material of choice for the fabrication of large load-bearing composites due to their high strength, superior stiffness, and low density; nonetheless, the mechanical strength of currently produced carbon fibers (~3–7 GPa) has only reached a small percentage of the theoretically predicated value (~180 GPa) due to the presence of structural defects and/or inhomogeneities [1,2]. The relatively large diameter of PAN precursor fibers (~8–15 μm) is one of the fundamental reasons responsible for the formation of structural imperfections [3], while the conventional spinning methods (such as wet spinning and air-gap spinning) are difficult and/or expensive, if not impossible, to produce PAN precursor fibers with diameters that are orders of magnitude smaller than 10 μm.

The technique of electrospinning provides a straightforward approach for the preparation of fibers with diameters ranging from sub-microns to nanometers [4–7]. The electrospun PAN nanofibers described herein are morphologically and structurally uniform, and their diameters are ~300 nm [8]. Such diameters are about 30 times thinner than those of the conventional PAN precursor fibers. The electrospun PAN nanofibers possess high degrees of macromolecular orientations and substantially reduced concentration of structural defects, and the ultra-small diameters may also mitigate the formation of structural inhomogeneities, particularly sheath-core structures, during the thermal treatments [3,9–11]. Unlike carbon nanofibers developed from the bottom-up synthetic method of chemical vapor deposition [12], electrospun carbon nanofibers are produced through a top–down nano-manufacturing process; therefore, they are low-cost, continuous, and also easy to align, assemble, and process into applications.

Although several research efforts have been devoted to the development of electrospun PAN based carbon nanofibers in recent years [4,8,10,11], the reported values of mechanical strength are far below the predictions. This is primarily due to the following reasons: (1) Randomly overlaid nanofiber mats instead of highly aligned nanofiber bundles were used as precursors, thus tension could not be applied effectively to individual nanofibers during the oxidative stabilization in air. It is known that applying tension during stabilization is crucial for preparing high performance carbon fibers; if the stabilization is carried out without tension, the

* Corresponding author. Tel.: +86 791 812 0389; fax: +86 791 812 0536.
** Corresponding author. Tel.: +1 605 394 1229; fax: +1 605 394 1232.
E-mail addresses: haoqing@jxnu.edu.cn (H. Hou), Hao.Fong@sdsmt.edu (H. Fong).

0032-3861/$ – see front matter © 2010 Elsevier Ltd. All rights reserved.
doi:10.1016/j.polymer.2010.03.044

resulting carbon fibers will be mechanically weak. (2) The electrospun carbon nanofibers were prepared without optimization of the processing conditions during electrospinning the precursor fibers and the subsequent thermal treatments, and the carbonization was conducted in the relatively low temperature range of below 1200 °C. For example, the oxidative stabilization of PAN precursor fibers occurs in air, and the process is strongly influenced by diffusion of oxygen molecules and stabilization byproducts [1,2]. The incorporation of small amounts of stabilization promoters (such as heteropolyacids [13,14]) into precursor fibers, as well as aligning and stretching the precursor fibers [15,16], can considerably facilitate the stabilization process and result in the formation of carbon fibers with higher mechanical strength.

In this study, systematic investigations were carried out to prepare uniform (*i.e.*, without beads and/or beaded nanofibers [17]) PAN nanofibers with diameters ranging from 250 nm to 350 nm. The nanofibers contained small amounts (1–5 wt.%) of phosphoric acid (PA) as the stabilization promoter, and they were collected as bundles of aligned nanofibers using a specially designed rotating disk; the aligned PAN nanofiber bundles were then used as the innovative precursors for the development of graphitic carbon nanofibers (GCNFs). It is noteworthy that, the PAN nanofiber bundles were tightly wrapped onto ceramic rods prior to thermal treatments; thus tension existed in individual nanofibers during the stabilization in air. This was because the precursor fibers tended to contract during the oxidative stabilization. Although tension was not applied during the subsequent carbonization and graphitization, it is known that applying tension during stabilization reduces the need for tension during carbonization and graphitization [1,2]. The results indicated that PA functioned as an effective promoter during the formation of ordered graphitic structures in the nanofibers, and the GCNFs made from the electrospun PAN precursor nanofibers containing 1.5 wt.% of PA exhibited the mechanical strength that was 62.3% higher than that of the GCNFs made from the precursor nanofibers without PA.

2. Experimental

2.1. Materials

PAN (M_w = 150,000 g/mol, catalog number: 181315) and *N,N*-dimethylformamide (DMF, catalog number: 227056) were purchased from the Sigma–Aldrich Co. (St. Louis, USA). Phosphoric acid (PA) was purchased from the Jing-Hua Scientific and Technological Research Institute (Shanghai, China). The materials were used without further purification.

2.2. Electrospinning and collection of aligned PAN nanofiber bundles

Numerous solutions (spin dopes) with varied concentrations of PAN and PA as well as different processing conditions and procedures of electrospinning were investigated during this study; the optimal ones based upon morphologies, structures, and mechanical properties of the resulting GCNFs are reported as follows: PAN was first dissolved in DMF to prepare 10 wt.% solutions, PA was then added into the solutions with weight fractions being 1.0%, 1.5%, 2.0%, 3.0%, 4.0%, and 5.0% of PAN to make spin dopes. Subsequently, each spin dope was placed into a 30 ml plastic syringe with a blunt-end stainless steel needle having an inside diameter of 0.55 mm. The needle was connected to a positive high voltage power supply purchased from the Gamma High Voltage Research, Inc. (Ormond Beach, USA). A laboratory-produced aluminum disc with the diameter of 30 cm and the rim width of 8 mm was placed 20 cm below the tip of the needle as the nanofiber collector (Fig. 1). During electrospinning, a positive high voltage of 20 kV was applied to the needle, while a negative high voltage of 10 kV was applied to the metal disc. The feed rate of spin dope was set at 1.5 ml/h using a KDS 200 syringe pump purchased from the KD Scientific Inc. (Holliston, USA). Electrospun PAN nanofibers were collected on aluminum foil that covered the rim. The linear speed at the rim surface was 32 m/s. After electrospinning, the aligned PAN nanofiber bundles were peeled from the aluminum foil and then dried at 60 °C in a vacuum oven for 4 h prior to the stabilization treatment. All of the prepared bundles had a thickness of ~30 μm and a mass per unit area of ~10 g/m^2.

2.3. Stabilization, carbonization, and graphitization

The stabilization and carbonization were conducted in a Lindberg 54 453 heavy duty tube furnace purchased from the TPS Co. (Watertown, USA). Prior to stabilization, the electrospun PAN nanofiber bundles were tightly wrapped onto ceramic rods with the diameter of 2 cm; therefore, tension existed in individual nanofibers because the fibers tended to contract during the oxidative stabilization in air. The wrapped PAN nanofiber bundles were heated to 230 °C at a heating rate of 2 °C/min in a constant flow of air, the temperature was then held at 230 °C for 3 h. The stabilized nanofiber bundles were subsequently un-wrapped and then heated at a rate of 2 °C/min to 1000 °C in argon followed by holding the temperature at 1000 °C for 1 h. The carbonized PAN nanofiber bundles were further graphitized in vacuum (~6 Pa) at 2200 °C for 2 h to develop GCNFs in a Lindberg high temperature reactor with inside diameter and depth being 12 cm and 25 cm, respectively; and the heating rate during graphitization was 5 °C/min.

2.4. Characterization and evaluation

A JSM-7500F scanning electron microscope (SEM) was used to observe morphologies of GCNFs at an acceleration voltage of 20 kV. The structures of GCNFs were examined using a JEM-2010 transmission electron microscope (TEM). TEM specimens were prepared by dispersing the nanofibers onto lacey carbon films, which were supported on 200-mesh copper grids. The structures of GCNFs were also studied with a Siemens D5000 X-Ray diffractometer (XRD), a LabRAM HR-800 Raman spectrometer using an excitation laser with the wavelength of 632.8 nm, and a Bruker Tensor-27 Fourier transform infrared spectrometer (FT-IR). The XRD specimens were prepared on rectangular glass slides with the aligning direction of nanofibers perpendicular to the scanning direction of X-ray beam. The X-ray tube operating at 40 kV and 40 mA with the CuKα radiation (λ = 0.154 nm) was used; and XRD profiles were recorded at the 2θ angles ranging from 10° to 60° at a scanning speed of 6 °C/min. The FT-IR specimens were prepared by grinding and pressing the nanofibers with anhydrous KBr, while the Raman analyses were carried out using GCNF bundles directly. The tensile strengths of GCNF bundles were measured using a computer-controlled SANS CMT-8102 mechanical testing machine at a crosshead speed of 0.5 mm/min. The weight losses of the stabilized PAN nanofibers, from room temperature to 800 °C in nitrogen, were recorded using a Shanghai WRP-3P thermal gravimetric analyzer (TGA) at a heating rate of 10 °C/min.

3. Results and discussion

3.1. Morphologies and structures

SEM images in Fig. 2 showed the representative morphologies of GCNFs made from the precursors of electrospun PAN nanofiber bundles with the PA weight fractions of 0%, 1.5%, 3.0% and 5.0%. It

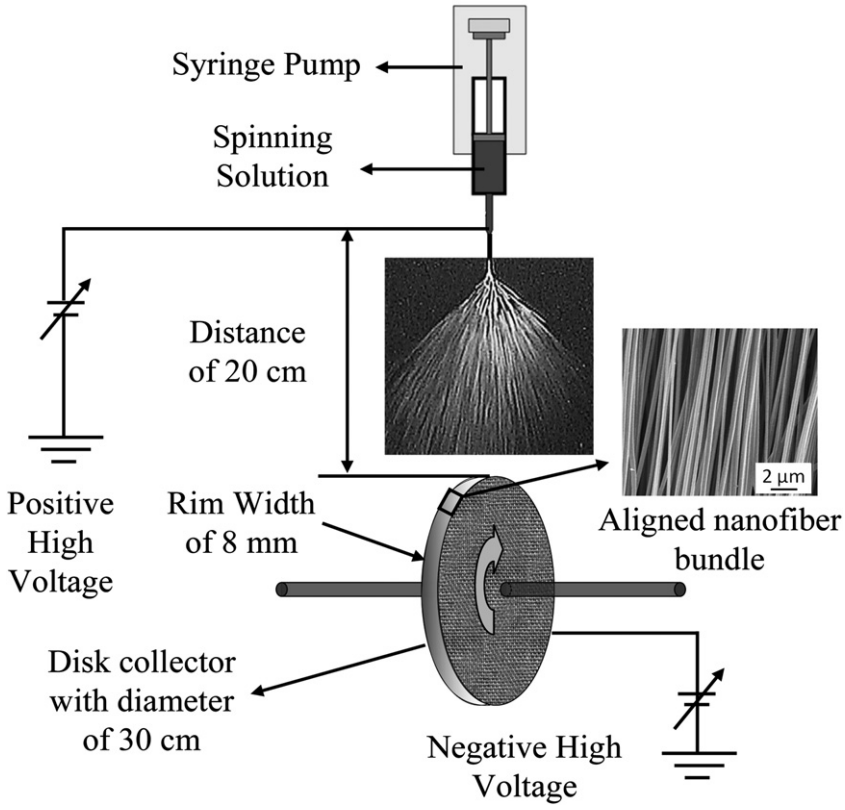

Fig. 1. Schematic representation of the electrospinning setup.

was evident that the designed rotating disk resulted in a reasonably high degree of nanofiber alignments; additionally, all GCNFs were without beads and/or beaded nanofibers [17], and their diameters ranged from 250 nm to 350 nm. It was known that ions in spin dopes increased the amounts of excess charges in the electrospinning filaments and thereby resulted in the reduction of nanofiber diameters [17]; the similar diameters of GCNFs made from the precursor fibers with varied PA weight fractions suggested that the majority of PA in the spin dopes existed as molecules instead of ions.

High resolution TEM images in Fig. 3 showed the graphitic structures in GCNFs. It was evident that the graphitization at 2200 °C resulted in the formation of graphene sheets that were stacked together into ribbon-shaped structures. In the GCNFs made from the neat PAN nanofibers (without PA), the graphene sheets in the ribbon-shaped structures were neither perfectly parallel to each other nor perfectly aligned with the fiber axes, while structural defects and/or inhomogeneities such as irregularly oriented carbonaceous components could often be observed (images 3A and 3A′). Contrastively, in the GCNFs made from the PAN nanofibers containing 1.5 and 3 wt.% PA, the ribbon-shaped graphitic structures were much more parallel to each other as well as to the longitudinal axes of the fibers; much fewer structural imperfections could be microscopically identified within the scope of this study, and the areas with poorly developed graphene sheets were substantially smaller (images 3B and 3B′, images 3C and 3C′). However, when the PA content was further increased to 5 wt.%, the graphene sheets in the ribbon-shaped structures became less ordered; although the sizes of the structures appeared to be larger, some needle-like defects emerged (images 3D and 3D′). These results demonstrated that the presence of a small amount (*i.e.*, 3 wt.% or less) of PA in the precursor nanofibers effectively promoted the formation of ribbon-shaped graphitic structures that were oriented parallel to each other as well as to the fiber axes; nonetheless, a large amount (*i.e.*, 5 wt.% or more) of PA led to the formation of structural imperfections.

XRD analyses were then carried out to further investigate the crystalline structures in the prepared GCNFs. The three diffraction peaks in Fig. 4 centered at 2θ angles of 26°, 43°, and 54° were attributed to the crystallographic planes of (002), (100), and (004) in graphitic structure, respectively [18,19]. The average interplanar spacing "$d_{(002)}$", calculated by the Bragg equation, decreased from 0.342 nm to 0.339 nm, after 1.5 wt.% of PA was added into the precursor nanofibers; while no more appreciable decrease of the $d_{(002)}$ value was observed with further increase of PA contents to 2.0, 3.0, 4.0, and 5.0 wt.%. Since the "$d_{(002)}$" value for naturally occurring graphite crystals is 0.335 nm [18], the GCNFs made from PA-containing PAN nanofibers possessed graphitic structures that resembled those in natural graphite with a higher degree. Additionally, the average width (size) and thickness parameters "L_a" and "L_c" of graphitic crystallites in the GCNFs could arguably be determined using the Scherrer equation; and the values of "L_a", and "L_c" became distinctly larger after 1.5 wt.% of PA was added to the precursor nanofibers. These results further suggested that PA was an effective promoter for the formation of ordered graphitic structures in GCNFs.

Raman spectroscopy is another powerful instrumentation to study the microstructures in carbonaceous materials [20,21]. The Raman spectra of carbonaceous materials have two characteristic bands including (1) "D-band", centered at the Raman shift of 1340 cm^{-1} and related to disordered turbostratic structures, and (2) "G-band", centered at the Raman shift of ~1580 cm^{-1} and related to ordered graphitic structures. The intensity ratio of the "D-band" to the "G-band" ("I_D/I_G", known as the "*R*-value") indicates the amount of structurally ordered graphite crystallites in the carbonaceous materials. *R*-values of the prepared GCNFs decreased from 1.25 to 0.66 as the PA weight fraction in the precursor nanofibers

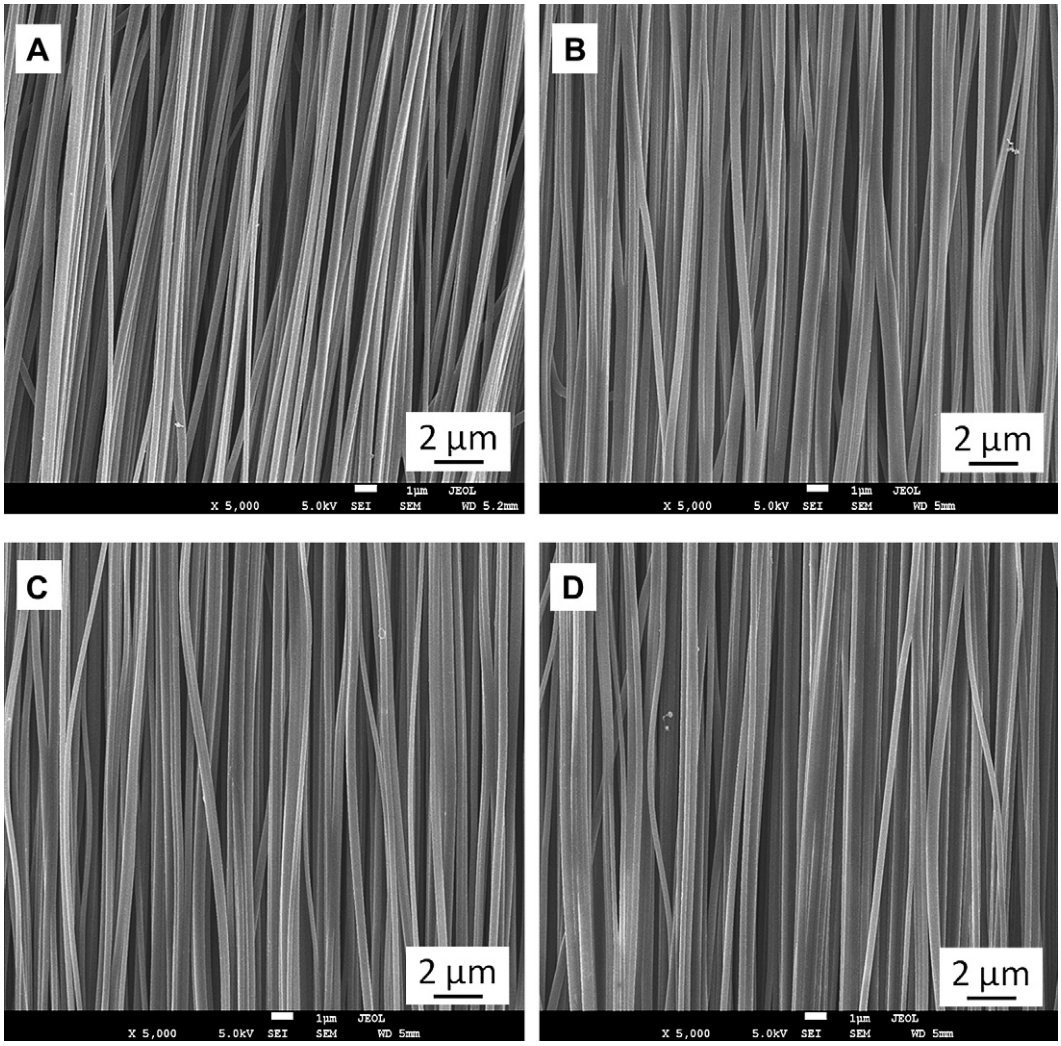

Fig. 2. SEM images showing the morphologies of GCNFs made from electrospun PAN nanofiber bundles with PA weight fractions being (A) 0%, (B) 1.5%, (C) 3.0%, and (D) 5.0%.

increased from 0% to 5% (Fig. 5); this once again indicated that the presence of PA promoted the formation of ordered graphitic structures in GCNFs.

3.2. Mechanical properties

As shown in Fig. 6, the GCNF bundles made from the electrospun PAN precursor nanofibers without PA had an average tensile strength of 597 MPa, while the addition of 1.5 wt.% PA into the precursor nanofibers increased the average tensile strength to 969 MPa; this represented an improvement of 62.3%. Nonetheless, the increase of PA content to 5 wt.% did not further improve the tensile strength; instead, the average tensile strength of the GCNF bundles decreased to 760 MPa. These data were consistent with the changes in morphological structures of the GCNFs observed in the TEM, XRD, and Raman studies. It is noteworthy that, although nanofibers in the bundles were aligned, the degrees of alignment were not extremely high; this is due to the reason that the formation of electrospun nanofibers is resulted from "bending instability" [7], which makes the traveling trajectory of an electrospinning filament very complicated; the rotating disk (or similar devices) is able to render a certain degree of nanofiber alignment, while such an alignment is far from perfect. Therefore, the strength of GCNF bundles is determined not only by the strength of individual nanofibers but also the entanglements and/or interactions among the nanofibers at contacting locations. In this study, all GCNF bundles had similar morphologies; presumably, they also had similar entanglements and/or interactions among the nanofibers. The strength differences of GCNF bundles were thus attributed to the different graphitic structures that resulted from the different amounts of PA in the precursor nanofibers. Based upon the acquired results, the PA weight fraction of ~1.5% in electrospun PAN precursor nanofibers appeared to be optimal. It is noteworthy that the strength values obtained from the measurements of nanofiber bundles cannot be interpreted directly as the strength values of individual nanofibers, since not all the fibers broke at the same stain level in such tensile tests. There is the likelihood that the strength of individual nanofibers is several to 100 times higher than that of the bundles [22,23]. Direct measurements of individual GCNFs can be accomplished with a special electronic single-filament tensile tester, which is currently being constructed. Additionally, as compared to the GCNFs made from the electrospun PAN precursor nanofibers without PA, the GCNFs made from the precursor nanofibers with PA had slightly larger values of deformation at break; for example, the value of deformation at break for the GCNFs made from the electrospun PAN precursor nanofiber with 1.5 wt.% PA was 1.79% higher. While the detailed reasons are upon further investigations, we believe that the highly ordered

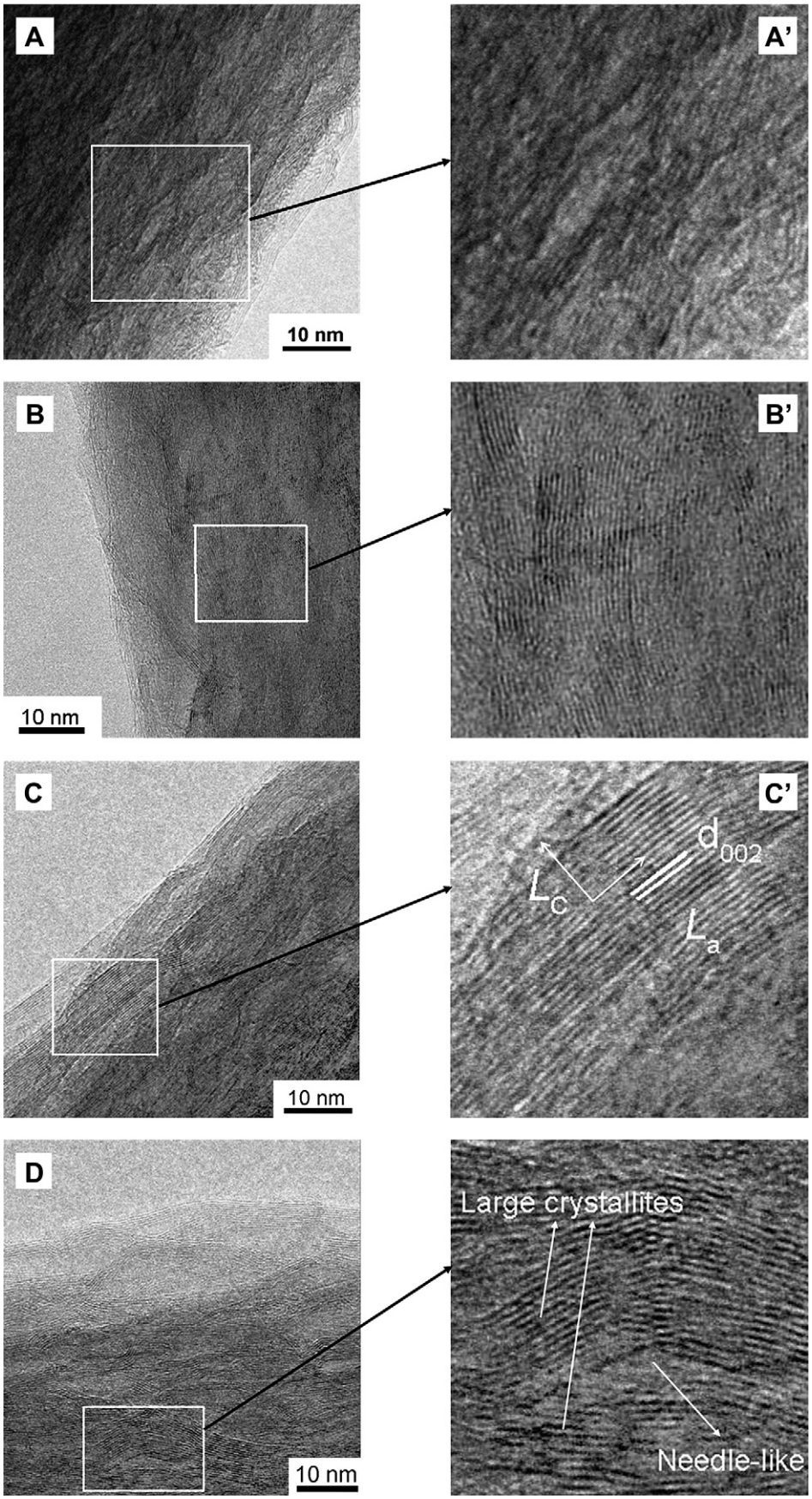

Fig. 3. TEM images showing the graphitic structures in GCNFs made from electrospun PAN nanofiber bundles with PA weight fractions being (A) 0%, (B) 1.5%, (C) 3.0%, and (D) 5.0%.

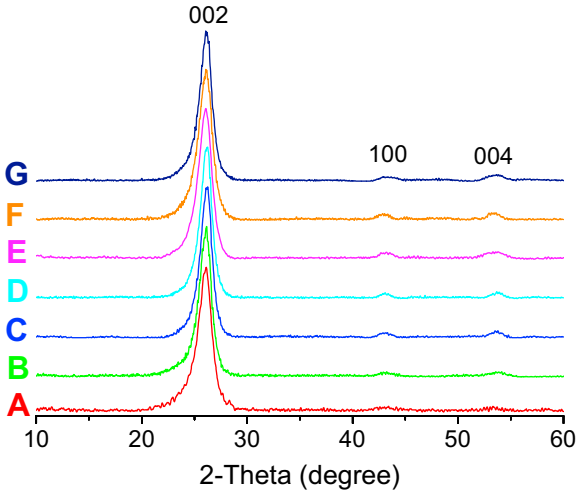

Fig. 4. XRD curves of GCNFs made from bundles of electrospun PAN nanofibers with PA weight fractions being (A) 0%, (B) 1.0%, (C) 1.5%, (D) 2.0%, (E) 3.0%, (F) 4.0%, and (G) 5.0%.

graphitic structures and/or the substantially reduced defect amounts might have important contributions (see the following Results And Discussion).

3.3. Functions of PA during thermal treatments

The above results clearly demonstrated that the presence of PA in the electrospun PAN precursor nanofibers facilitated the formation of ordered graphitic structures in GCNFs. Previous research efforts indicated that PA possessed the capability to promote the development of cyclic and/or aromatic structures during thermal treatments of wood, Nomex, coal, and PAN [24–27]. To understand the detailed functions of PA during the thermal treatments (particularly the oxidative stabilization in air) of the electrospun PAN precursor nanofibers, FT-IR and TGA analyses were carried out. As compared to the FT-IR spectrum of the stabilized PAN nanofibers without PA (curve "A" in Fig. 7), the spectrum of the stabilized PAN nanofibers containing 1.5 wt.% of PA (curve "B" in Fig. 7) had significantly lower intensities of (1) "C≡N" band centered at the wavenumber of 2240 cm^{-1} and (2) "C–H" band in the "$-CH_2-$" structure centered at the wavenumber of 1450 cm^{-1},

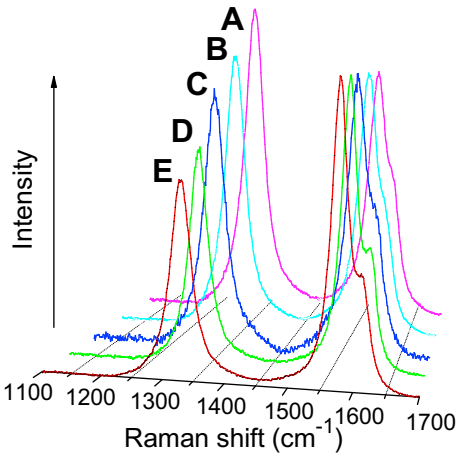

Fig. 5. Raman spectra of GCNFs made from bundles of electrospun PAN nanofibers with PA weight fractions being (A) 0%, (B) 1.5%, (C) 3.0%, (D) 4.0%, and (E) 5.0%.

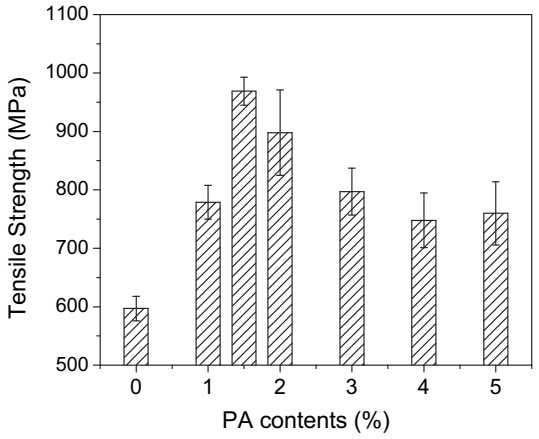

Fig. 6. Tensile strengths of GCNF bundles made from electrospun PAN nanofiber bundles with varied weight fractions of PA. Each datum is the mean value of six measurements with the error bar representing one standard deviation.

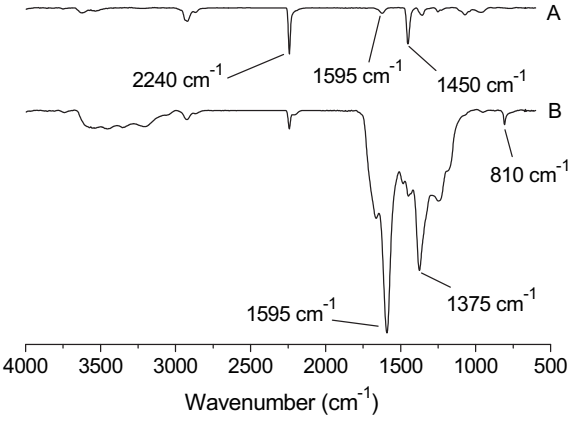

Fig. 7. FT-IR spectra of the stabilized electrospun PAN nanofibers without (curve "A") and with (curve "B") 1.5 wt.% of PA.

while it had significantly higher intensities of (1) "C=N" band centered at the wavenumber of 1595 cm^{-1} and (2) "C–H" band in the "=CH–" structure centered at the wavenumber of 1375 cm^{-1}. Additionally, the emerging band centered at the wavenumber of 810 cm^{-1} indicated that aromatic structures started to form in the stabilized PAN nanofibers with PA; and this band was attributed to the vibration motion of "C–H" bond in aromatic structures [24].

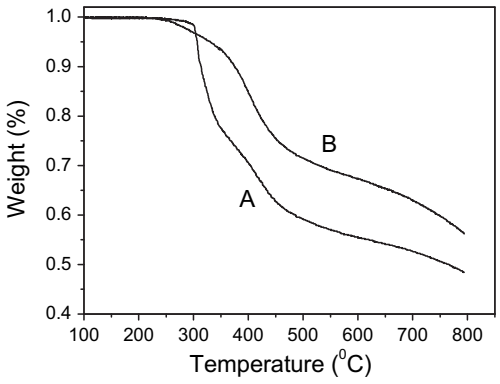

Fig. 8. TGA curves of the stabilized electrospun PAN nanofibers with (curve "B") and without (curve "A") 1.5 wt.% of PA. The TGA experiments were carried out in nitrogen.

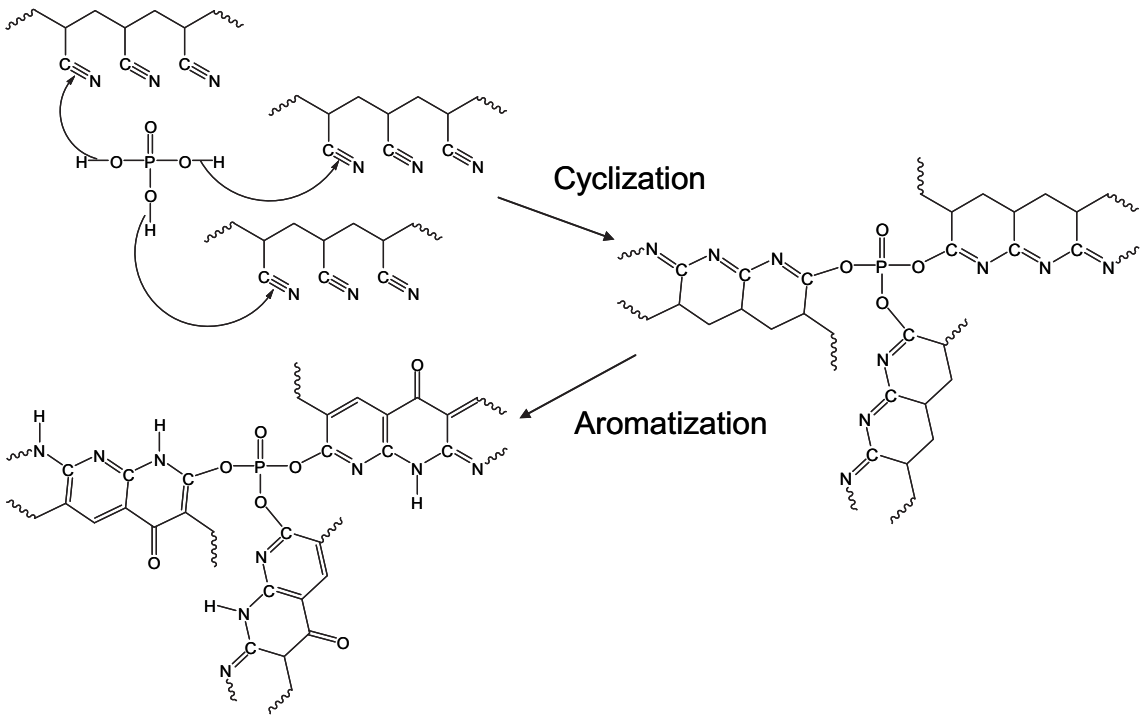

Fig. 9. Schematic diagram depicting PA's functions during the stabilization of PAN in air.

The temperature dependences of weight losses in nitrogen environment for the stabilized PAN nanofibers with (curve "B") and without (curve "A") 1.5 wt.% PA were shown in Fig. 8. The weight losses in TGA analyses, particularly under 600 °C, simulated what would occur during carbonization of the stabilized PAN fibers [24]. It was evident that the stabilized PAN nanofibers with 1.5 wt.% of PA were more stable (*i.e.,* well-stabilized) and achieved a higher carbon yield than the PAN nanofibers without PA. The temperature for 10% weight loss of the stabilized PAN nanofibers with PA was ~370 °C, which was ~50 °C higher than that of the PAN nanofibers without PA. The remaining weight at 800 °C for the nanofibers with PA was ~20% higher than that of the nanofibers without PA. Intriguingly, the stabilized PAN nanofibers with PA started the weight loss at a temperature ~50 °C lower than the nanofibers without PA. Such a weight loss was attributed to further aromatization of the cyclic structures in the stabilized PAN [24], suggesting that the PA-containing nanofibers were well-stabilized and had a higher tendency to undergo the further aromatization.

It was reported that the cyclization of PAN macromolecules could be initiated by the functional groups of carboxyl and/or hydroxyl through the reduction of activation energy for the reaction [28,29]. PA molecules in the electrospun PAN precursor nanofibers could effectively initiate the cyclization and further induce the aromatization, as schematically shown in Fig. 9; and this was evidenced by the FT-IR and TGA results. The well-stabilized PAN nanofibers possessed regularly oriented ladder structures, which further facilitated the formation of ordered graphitic structures in the final GCNFs as supported by the TEM, XRD, and Raman results. It is noteworthy that after carbonization and graphitization, hetero-atoms including phosphorus, oxygen, and nitrogen no longer exist in the GCNFs. If the amount of PA in the precursor nanofibers was too high (*e.g.,* 5 wt.%), however, the PA would result in the formation of needle-like defects, leading to lower mechanical strength. This was because a high amount of PA in a spin dope would probably form PA-enriched phases due to low miscibility and/or compatibility between PAN and PA, such phases would be elongated during the electrospinning process (particularly during the "bending instability" [7]) and would further result in the generation of PA-enriched needle-like domains in the precursor nanofibers; after thermal treatments, these domains would eventually become the needle-like defects in GCNFs. When the PA content was optimal (*e.g.,* 1.5 wt.%), PA could effectively promote the formation of ordered graphitic structures in GCNFs without generation of needle-like defects; therefore, the GCNFs developed from the electrospun PAN precursor nanofibers with 1.5 wt.% of PA demonstrated the highest mechanical strength.

4. Conclusions

In this study, bundles of aligned electrospun PAN nanofibers containing varied amounts of PA were prepared and used as innovative precursors for the development of GCNFs through thermal treatments including stabilization in air, carbonization in argon, and graphitization in vacuum. The developed GCNFs were morphologically uniform with diameters of ~300 nm; and the GCNFs made from the PAN precursor nanofibers containing 1.5 wt.% of PA exhibited the mechanical strength that was 62.3% higher than the GCNFs made from the precursor nanofibers without PA. PA molecules in the electrospun PAN precursor nanofibers effectively initiated the cyclization and induced the aromatization during the oxidative stabilization, as indicated by the FT-IR and TGA results. The well-stabilized PAN nanofibers possessed regularly oriented ladder structures, which facilitated the further formation of ordered graphitic structures in GCNFs during the subsequent carbonization and graphitization, as supported by the TEM, XRD, and Raman results. The GCNFs are expected to have important applications including the development of nanocomposites.

Acknowledgements

HH thanks the support from the National Natural Science Foundation of China (Grants No.: 20674034 and 20874041), the

Ministry of Education of China (Grant No.: 707038), and the Bureau of Science and Technology of Jiangxi Province in China (Grant No.: 050008). HF thanks the support from the National Aeronautics and Space Administration of the United States (Grant No.: NNX07AT52A), the Department of Energy in the United States (Grant No.: DE-FG02-08ER64624), and the National Science Foundation of the United States (Grant No. CBET-0827844).

References

[1] Donnet JB, Wang TK, Peng JC, Rebouillat S. Carbon fibers. New York, NY: Marcel Dekker; 1998. p. 231–309.
[2] Morgan PE. Carbon fibers and their composites. Boca Raton, FL: CRC Press; 2005. p. 185–267.
[3] Liu J, Yue Z, Fong H. Continuous nanoscale carbon fibers with superior mechanical strength. Small 2009;5(5):536–42.
[4] Chun I, Reneker DH, Fong H, Fang X, Deitzel J, Beck-Tan N, et al. Carbon nanofibers from polyacrylonitrile and metaphase pitch. Journal of Advanced Materials 1999;31(1):36–41.
[5] Reneker DH, Chun I. Nanometer diameter fiber of polymer, produced by electrospinning. Nanotechnology 1996;7(3):216–23.
[6] Dzenis Y. Spinning continuous fibers for nanotechnology. Science 2004;304 (5679):1917–9.
[7] Fong H. Electrospun polymer, ceramic, carbon/graphite nanofibers and their applications, vol. 2. Stevenson Ranch, CA: American Scientific Publishers; 2007. p. 451–74.
[8] Liu J, Zhou P, Zhang L, Ma Z, Liang J, Fong H. Thermo-chemical reactions occurring during the oxidative stabilization of electrospun polyacrylonitrile precursor nanofibers and the resulting structural conversions. Carbon 2009;47 (4):1087–95.
[9] Greiner A, Wendorff JH. A fascinating method for the preparation of ultrathin fibers. Angewandte Chemie – International Edition 2007;46(30):5670–703.
[10] Gu SY, Ren J, Vancso GJ. Process optimization and empirical modeling for electrospun polyacrylonitrile (PAN) nanofiber precursor of carbon nanofibers. European Polymer Journal 2005;41(11):2559–69.
[11] Moon SC, Farris RJ. Strong electrospun nanometer-diameter polyacrylonitrile carbon fiber yarns. Carbon 2009;47(12):2829–39.
[12] Yu MF, Lourie O, Dyer MJ, Moloni K, Kelly TF, Ruoff RS. Strength and breaking mechanism of multi-walled carbon nanotubes under tensile load. Science 2000;287(5453):637–40.
[13] Nataraj S, Kim B, Yun J, Lee D, Aminabhavi T, Yang K. Effect of added nickel nitrate on the physical, thermal and morphological characteristics of polyacrylonitrile-based carbon nanofibers. Materials Science and Engineering: B 2009;162(2):75–81.
[14] Nataraj SK, Kim BH, Yun JH, Lee DH, Aminabhavi TM, Yang KS. Morphological characterization of electrospun carbon nanofiber mats of polyacrylonitrile containing heteropolyacids. Synthetic Metals 2009;159(14):1496–504.
[15] Wu S, Zhang F, Yu Y, Li P, Yang X, Lu J, et al. Preparation of PAN-based carbon nanofibers by hot-stretching. Composite Interfaces 2008;15(7–9):671–7.
[16] Zhou ZP, Lai CL, Zhang LF, Hou HQ, Reneker DH, Fong H. Development of carbon nanofibers from aligned electrospun polyacrylonitrile nanofiber bundles and characterization of their microstructural, electrical, and mechanical properties. Polymer 2009;50:2999–3006.
[17] Fong H, Chun I, Renker DH. Beaded nanofibers formed during electrospinning. Polymer 1999;40(16):4585–92.
[18] Zussman E, Chen X, Ding W, Calabri L, Dikin DA, Quintana JP, et al. Mechanical and structural characterization of electrospun PAN-derived carbon nanofibers. Carbon 2005;43(10):2175–85.
[19] Iwashita N, Park CR, Fujimoto H, Shiraishi M, Inagaki M. Specification for a standard procedure of X-ray diffraction measurements on carbon materials. Carbon 2004;42(4):701–14.
[20] Jawhari T, Roid A, Casado J. Raman spectroscopic characterization of some commercially available carbon black materials. Carbon 1995;33(11):1561–5.
[21] Endo M, Kim C, Karaki T, Kasai T. Structural characterization of milled mesophase pitch-based carbon fibers. Carbon 1998;36(11):1633–41.
[22] Harrison D. Synthetic fibers for nonwovens update. Nonwoven Industry 1997;28(6):32–9.
[23] Michielsen S, Pourdeyhimi B, Desai P. Review of thermally point-bonded nonwovens: materials, processes, and properties. Journal of Applied Polymer Science 2006;99(5):2489–96.
[24] Solum MS, Pugmire RJ, Jagtoyen M, Derbyshire F. Evolution of carbon structure in chemically activated wood. Carbon 1995;33(9):1247–54.
[25] Suarez-Garcia F, Martinez-Alonso A, Tascon JMD. Beneficial effects of phosphoric acid as an additive in the preparation of activated carbon fibers from Nomex aramid fibers by physical activation. Fuel Processing Technology 2002;77–78:237–44.
[26] Toles C, Rimmer S, Hower JC. Production of activated carbons from a Washington lignite using phosphoric acid activation. Carbon 1996;34(11): 1419–26.
[27] Sun J, Wu L, Wang Q. Comparison about the structure and properties of PAN-based activated carbon hollow fibers pretreated with different compounds containing phosphorus. Journal of Applied Polymer Science 2005;96 (2):294–300.
[28] Zhang L, Hsieh Y-L. Nanoporous ultrahigh specific surface polyacrylonitrile fibres. Nanotechnology 2006;17:4416–23.
[29] Kim J, Kim YC, Ahn W, Kim CY. Reaction mechanisms of polyacrylonitrile on thermal treatment. Polymer Engineering and Science 1993;33(22):1452–7.